Thermochimica Acta 489 (2009) 70–74

Contents lists available at ScienceDirect

Thermochimica Acta

journal homepage: www.elsevier.com/locate/tca

Entropy generation during a phase-change process in a parallel plate channel

Mehmet F. Orhan[a], Aytunc Erek[b,*], Ibrahim Dincer[a]

[a] Faculty of Engineering and Applied Science, University of Ontario Institute of Technology (UOIT), 2000 Simcoe Street North, Oshawa, Ontario L1H 7K4, Canada
[b] Department of Mechanical Engineering, Dokuz Eylul University, Bornova 35100, Izmir, Turkey

ARTICLE INFO

Article history:
Received 31 October 2008
Received in revised form 3 February 2009
Accepted 4 February 2009
Available online 13 February 2009

Keywords:
Entropy
Energy
Thermodynamics
Phase change
Heat conduction

ABSTRACT

This study addresses the entropy generation in heat conduction, accompanied by melting/solidification. The energy and entropy equations for one-dimensional transient thermal analysis with associated boundary and initial conditions are solved numerically using a fixed grid numerical model with the finite control volume approach following the Thomas algorithm. On the other hand, the dimensionless thermal conductivity, K, is calculated by harmonic mean method at the control surface. The numerical results are then verified by testing the resulting predictions for independence of the grid size, time-step and other parameters. Proper trends and a good agreement between the results of theoretical modeling and physical reality for the solidification/melting process are obtained. A parametric study with various associated parameters is performed and results are illustrated.

1. Introduction

Minimization of entropy generation, without sacrificing energetic efficiency, is a key towards optimal design of phase-change processes. During a phase-change process, energy is transferred to one side of the material and subsequently is removed from the other side of material. Depending on the energy input the substrate material can undergo multiple changes in phase over the thermal cycle. The second law of thermodynamics imposes strict limitations on the nature of energy flow under such conditions. Actually, the entropy generation turns out to be a key parameter in achieving the upper limit of thermodynamics performance of phase-change processes. Therefore, an entropy analysis of such processes may become fruitful for optimizing the process parameters, which accordingly provide a more stringent process control and reduce the associated costs.

Problems of heat transfer accompanied by melting or solidification (the Stefan problems) are of considerable interest in many areas of science and technology. Main efforts in studies of these problems have been devoted to analysis of the temperature/concentration fields and the interface motion and shape. In the last decade there have been attempts to reconsider phase-change problems in the general framework of irreversible thermodynamics. These works enable one to control systematically various physical assumptions used in specific models and also bring attention to such aspects of the phase-change processes as the rate of entropy production both in the bulk and at the phase-change front.

Phase-change processes have received much attention in recent years because of their wide range of applications, and commonly encountered in a large variety of thermal engineering applications ranging from the freezing of water in pipes and heat exchangers to solidification of castings and crystallization from liquid phase. In addition, freezing and thawing of water within foodstuff is of great importance in food processing operations, which are often carried out by placing objects in an air stream.

Freezing, melting, evaporation, and structural changes of a material are characterized by discontinuous changes in thermodynamic properties at some definite temperatures and pressures without change of chemical composition. These transitions are thus called changes in state of aggregation or phase-changes as distinct from chemical changes. Underestimating the heat capacity usually results in unsatisfactory operation, due to the impossibility of reaching the desired operating conditions. On the other hand, overestimation of the capacity results in excess plant capacity and unnecessarily high initial investment and amortization cost. That is why an accurate prediction of the transient heat transfer during such phase-changes is of paramount importance, since it is inescapably involved in establishing the system capacity.

Many solution methods have been developed handling the phase-change problems, depending on the problem characteristics and geometry. Many of these methods are numerical ones. Obtaining analytical solutions are very difficult because of the nonlinear characteristics of the phase-change problems. There are few exact solutions about moving boundary problems for only some idealized situations, subject to simple boundary and initial conditions [1]. An

* Corresponding author. Tel.: +90 232 3883138; fax: +90 232 3887868.
E-mail addresses: Mehmet.Orhan@uoit.ca (M.F. Orhan), Aytunc.Erek@deu.edu.tr (A. Erek), Ibrahim.Dincer@uoit.ca (I. Dincer).

0040-6031/$ – see front matter © 2009 Elsevier B.V. All rights reserved.
doi:10.1016/j.tca.2009.02.002

Nomenclature

Bi	Biot number, hl/k_s
C_p	specific heat ($J\,kg^{-1}\,K^{-1}$)
Fo	Fourier number, $\alpha t/l^2$
h	heat transfer coefficient ($W\,m^{-2}\,K^{-1}$)
k_l	thermal conductivity of liquid ($W\,m^{-1}\,K^{-1}$)
k_s	thermal conductivity of solid ($W\,m^{-1}\,K^{-1}$)
l	distance of plates (m)
t	time (s)
T_l	temperature of liquid phase (K)
T_m	melting temperature (K)
T_s	temperature of solid phase (K)
T_∞	ambient temperature (K)
x	distance (m)
X	x/l

Greek letters

α_l	thermal diffusivity of liquid phase ($m^2\,s^{-1}$)
α_s	thermal diffusivity of solid phase ($m^2\,s^{-1}$)
ρ	density ($kg\,m^{-3}$)

analytical solution for the temporal location of moving solid–liquid interface of a phase-change process, occurring in parallel plate channels has been presented by Sahin and Dincer [2].

For the situations for which the exact solutions are not available; approximate, semi-analytical and numerical methods have been used to solve the phase-change problems. These methods are explained in [3] with some examples, and analyzed in detail in the state-of-art review about the subject [4]. On the other hand, Crank [5] presents an elaborate collection of numerical methods used for these problems.

Fixed grid solutions for phase-change problems remove the need to satisfy conditions at the phase-change front and can be easily extended to multi dimensional problems. The two most important and widely used methods are enthalpy methods and temperature-based equivalent heat capacity methods. Enthalpy methods [6] are flexible and can handle phase-change problems occurring both at a single temperature and over a temperature range. The drawback of this method is that although the predicted temperature distributions and the melting fronts are reasonable, the predicted time history of the temperature at a typical grid point may have some oscillations. The temperature-based fixed grid methods [7,8] have no such time history problems and are more convenient with conjugate problems involving an adjacent wall.

Second law formulation was presented with predictive and corrective capabilities for the improvement of phase-change predictions in solid–liquid systems by Naterer [9]. Naterer also applied the downward concavity and compatibility properties of entropy in a discrete entropy based stability analysis. Naphon [10] theoretically studied the heat transfer characteristics and entropy generation of the double pass flat plate solar air heater with longitudinal fins. Similar fin geometry was studied in terms of the effect of entropy generation by Dağtekin et al. [11]. They concluded that both the entropy generation and the pumping power to heat transfer ratio increase in case of triangular fin as the fin angle is increased. Yılbas and Pakdemirli [12] investigated entropy generation in a circular pipe due to the flow of a non-Newtonian Fluid with variable viscosity. A latent thermal energy system integrated with solar air heating system was numerically modeled by Kousksou et al. [13]. Energy and exergy analysis were applied to study and optimize the proposed system in their study.

The objectives of this paper are to present a detailed analysis of entropy generation of a phase-change process in a parallel plate channel using a fixed grid numerical model, including associated parametric study.

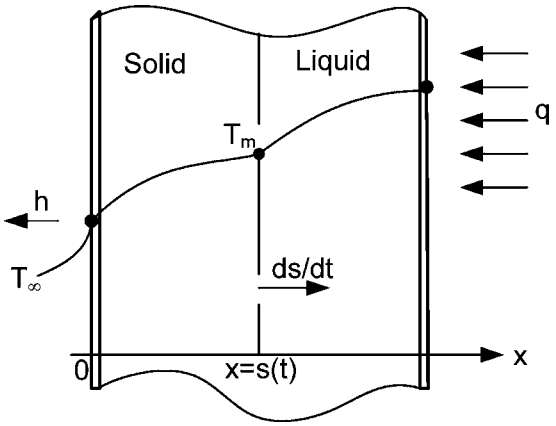

Fig. 1. Phase-change process in a parallel plate channel.

2. Problem statement

A one-dimensional rectangular enclosure of length L, filling a phase-change material (PCM) of the same size, is exposed to heat convection occurring from the flow of the cold fluid over its one wall. A constant heat flux, q, which would control of freezing process, is imposed on the other side wall of the enclosure illustrated in Fig. 1. The whole system is initially kept at the slightly over phase-change temperature, T_m. Namely, the system is at liquid phase initially.

The following assumptions are made for the analysis:

a) The physical properties are independent of the temperature and no density change occurs during the phase-change process.
b) The thicknesses of the plates are small and conductivity of their material is high so that the temperature drop across the plates can be neglected.
c) One side of the channel of width l is exposed to a cold ambient at time $t > 0$ and convection heat transfer takes place with a constant heat transfer coefficient, h. Thus, the solidification of the liquid with uniform initial temperature starts within the channel.
d) A constant heat flux, q, which would control the freezing process, is imposed on the other side of the channel.

The thermophysical properties of PCM are independent of temperature, but the properties of the PCM are different in the solid and liquid phases. Thermophysical properties of the PCM associated with the system can be found in Table 1.

Table 1
Thermophysical properties of water and geometrical parameters of PCM.

Parameter	Symbol	Value	Unit
Length of enclosure	L	0.1	m
Temperature difference	$\Delta T = T_m - T_\infty$	10 and 20	K
Biot number	Bi	10, 20 and 50	–
Phase-change temperature	T_m	273.15	K
Thermal conductivity of solid PCM	k_s	2.200	$W\,m^{-1}\,K^{-1}$
Thermal conductivity of liquid PCM	k_l	0.561	$W\,m^{-1}\,K^{-1}$
Density of solid	ρ_s	916.8	$kg\,m^{-3}$
Density of liquid PCM	ρ_l	999.8	$kg\,m^{-3}$
Specific heat of solid PCM	c_{ps}	2040	$J\,kg^{-1}\,K^{-1}$
Specific heat of liquid PCM	c_{pl}	4217	$J\,kg^{-1}\,K^{-1}$
Latent heat of fusion	ΔH	333, 500	$J\,kg^{-1}$

3. Analysis

The governing equation for energy is well known as one-dimensional heat conduction equation:

$$\frac{\partial(C\theta)}{\partial Fo} = \frac{\partial}{\partial X}\left(K\frac{\partial\theta}{\partial X}\right) \tag{1}$$

As the initial temperature of the system is considered to be the same or close to the phase-change temperature, the natural convection effect around the tube and fins can be neglected. The heat conduction in the PCM is described by a temperature transforming method using a fixed grid numerical model [7,8]. This model assumes that solidification process occurs over a range of phase-change temperature from $T_m - \delta T_m$ to $T_m + \delta T_m$, but it can also be successfully used to simulate solidification process occurring at a single temperature by taking a small range of phase-change temperature, $2\delta T_m$. The dimensionless energy equation for the PCM is written as

$$\frac{\partial(C\theta)}{\partial Fo} = \frac{\alpha_l}{\alpha_f}\left(\frac{1}{R}\frac{\partial}{\partial R}\left(KR\frac{\partial\theta}{\partial R}\right) + \frac{\partial}{\partial X}\left(K\frac{\partial\theta}{\partial X}\right)\right) - \frac{\partial S}{\partial Fo} \tag{2}$$

where

$$C = C(\theta) = \begin{cases} C_{sl} & \theta < -\delta\theta_m \quad \text{Solid phase} \\ \left(\frac{1}{2}(1+C_{sl}) + \frac{1}{2Ste\,\delta\theta_m}\right) & -\delta\theta_m \le \theta \le \delta\theta_m \quad \text{Mushy phase} \\ 1 & \theta > \delta\theta_m \quad \text{Liquid phase} \end{cases} \tag{3}$$

$$S = S(\theta) = \begin{cases} C_{sl}\delta\theta_m & \theta < -\delta\theta_m \quad \text{Solid phase} \\ \left(\frac{1}{2}\delta\theta_m(1+C_{sl}) + \frac{1}{2Ste}\right) & -\delta\theta_m \le \theta \le \delta\theta_m \quad \text{Mushy phase} \\ C_{sl}\delta\theta_m + \frac{1}{Ste} & \theta > \delta\theta_m \quad \text{Liquid phase} \end{cases} \tag{4}$$

$$K = K(\theta) = \begin{cases} K_{sl} & \theta < -\delta\theta_m \quad \text{Solid phase} \\ K_{sl} + \frac{(1-K_{sl})(T+\delta T^*)}{2\delta T^*} & -\delta\theta_m \le \theta \le \delta\theta_m \quad \text{Mushy phase} \\ 1 & \theta > \delta\theta_m \quad \text{Liquid phase} \end{cases} \tag{5}$$

The temperature distribution inside the solution domain can be calculated by solving the energy equations defined by Eqs. (1)–(5). The solution procedure used for solving these energy equation are the control volume approach described in [14]. On the other hand, the dimensionless thermal conductivity, K, is calculated by harmonic mean method at the control surface. Thomas algorithm is used for solving the discretization equations of energy equation.

Since energy equation for the PCM is a non-linear heat conduction equation, iterations are needed during each time step. For a given time step, convergence is declared at the $(k+1)^{\text{th}}$ iteration when $|\theta_{i,j}^{k+1} - \theta_{i,j}^{k}| \le 10^{-6}$. The numerical results are then verified by testing the resulting predictions for independence of the grid size, time-step and other parameters. The grid size used for the solution was 200 with a time step $\Delta\tau = 0.001$.

3.1. Entropy generation

After derivation of temperature change, now we can obtain a formulation for entropy generation rate. We regard the small element dx as a closed thermodynamic system subjected to energy transfer as shown in Fig. 2.

The element size is small enough so that the thermodynamic state of the fluid inside the element may be regarded as uniform (independent of position). However, the thermodynamic state of the element may be change with time. The fluid is in local thermodynamic equilibrium.

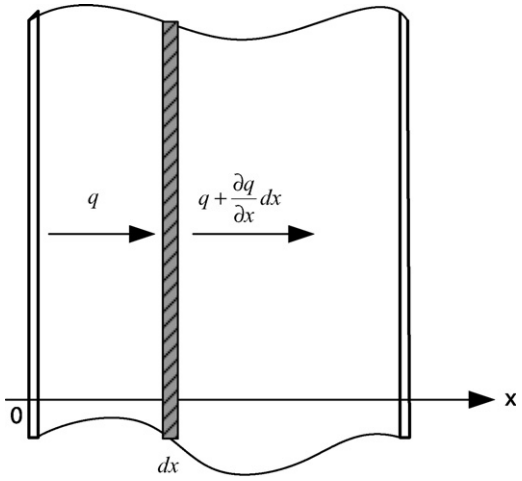

Fig. 2. Small element dx that exposed to heat flux in x direction.

Based on the above model, the entropy generation rate per unit volume $S'''_{gen} = [\mathrm{W\,m^{-3}\,K^{-1}}]$ may be estimated writing the second law of thermodynamics for dx as a closed system;

$$\dot{S}'''_{gen}\,\mathrm{d}x = \frac{q + (\partial q/\partial x)\,\mathrm{d}x}{T + (\partial T/\partial x)\,\mathrm{d}x} - \frac{q}{T} + \rho\frac{\partial s}{\partial t}\mathrm{d}x \tag{6}$$

In this expression the first two terms account for the entropy transfer associated with heat transfer, and the last term represents the rate of entropy accumulation in the element. Dividing Eq. (6) by dx, the local entropy generation becomes;

$$\dot{S}'''_{gen} = \frac{1}{T}\frac{\partial q}{\partial x} - \frac{q}{T^2}\frac{\partial T}{\partial x} + \rho\frac{\partial s}{\partial t} \tag{7}$$

And if $\partial s = \partial u/T$, where u is internal energy, inside the element dx

$$\rho\frac{\partial s}{\partial t} = \frac{\rho}{T}\frac{\partial u}{\partial t} \tag{8}$$

From the first law of thermodynamics, written for one point in the convective medium, $\rho(\partial u/\partial t) = -\partial q/\partial x$, so we can write down Eq. (8) as

$$\rho\frac{\partial s}{\partial t} = -\frac{1}{T}\frac{\partial q}{\partial x} \tag{9}$$

Combining Eq. (8) with Eq. (9) we obtain entropy generation as

$$\dot{S}'''_{gen} = -\frac{q}{T^2}\frac{\partial T}{\partial x} \tag{10}$$

Finally, if the Fourier law of heat conduction for an isotropic medium applies, $q = -k(\partial T/\partial x)$ the volumetric rate of entropy generation becomes

$$\dot{S}'''_{gen} = \frac{k}{T^2}\left(\frac{\partial T}{\partial x}\right)^2 \tag{11}$$

4. Results and discussion

One dimensional phase-change problem of water with the parameters given in Table 1 is investigated numerically. The relation between solidification fronts, S and dimensionless time, Fo is obtained as illustrated in Fig. 3. This figure shows that solidification fronts increase, following a concave down curve, with time. This growing of solidification fronts is continuous until it reaches 1, because we present it as a dimensionless parameter earlier. And also, as expected, the duration of complete solidification of channel increases while the heat flux on the hot site of channel is increased. This is because; the rate of solidification fronts is inversely proportional to the heat flux.

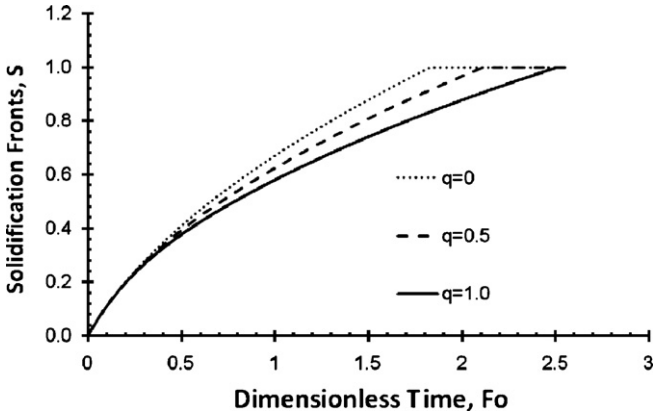

Fig. 3. Time variation of the solidification fronts for $Bi = 10$ and $T_m - T_\infty = 10$ K.

In Fig. 4, the temperature distribution is illustrated at different dimensionless time *Fo*. Temperature is negative at solid phase side and it is increasing towards the liquid phase side, as a result of heat flux on the right hand side. It reaches the melting temperature of "$T_m = 0\,^\circ$C" at inter-phase following a linear grade in solid phase, while following an increasing rate curve at liquid phase. At the same time the interface moving towards the positive *x* direction with time, while surface temperature of liquid side is decreasing. These results are based on the Biot number, $Bi = 10$ and temperature difference, $\Delta T = 10$ K as shown in the figure.

The relation between solidification fronts, *S* and dimensionless time, *Fo* with different Biot number, *Bi* and temperature difference, ΔT is given in Fig. 5. At constant temperature difference of $\Delta T = 10$ K, the solidification fronts is increasing with time as a concave down curve. And the rising rate of this curve is escalating when increasing Biot number. On the other hand, at the constant Biot number the solidification fronts increases while the temperature difference ΔT increases. In short, the solidification takes place faster when environment temperature T_∞ at cold side of channel decreased. And also the same effect can be seen when convection heat transfer coefficient *h* is increased and/or thermal conductivity *k* is decreased. Because, the convection is domain heat transfer type in the cold side of channel, while conduction is for hot side.

In Fig. 6, the relation between entropy generation, S_{gen} and dimensionless time, *Fo*, with different heat flux, is illustrated. Entropy generation increases abruptly at the beginning and makes

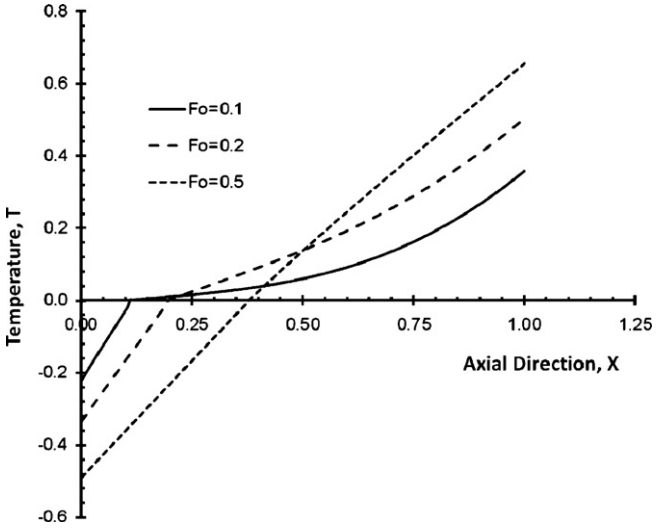

Fig. 4. Temperature distrubition with axial direction for $Bi = 10$ and $T_m - T_\infty = 10$ K.

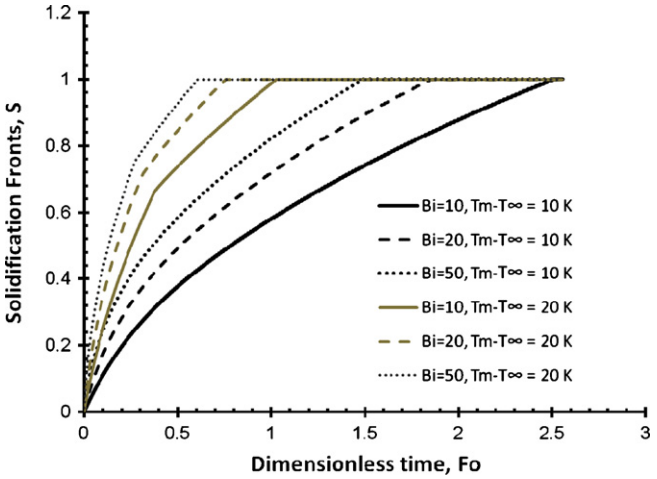

Fig. 5. Time variation of the solidification fronts.

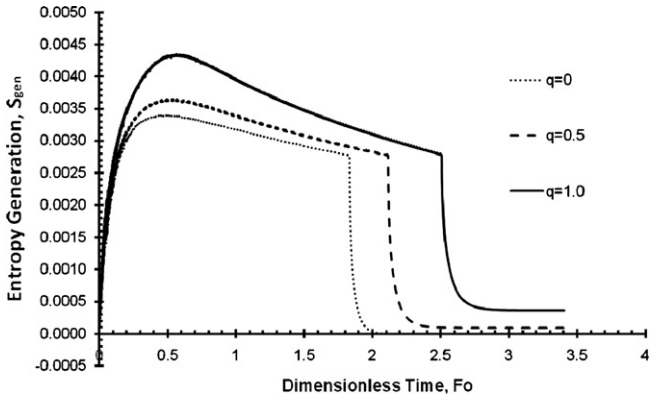

Fig. 6. The entropy generation with time for $Bi = 10$ and $T_m - T_\infty = 10$ K.

peak at $Fo = 0.5$ which is interphase point as it can be seen from the previous figures. By considering Eq. (10), it is seen that the volumetric rate of entropy generation depends on both temperature gradient and heat transfer rate. At the final stages of solidification process, the solidification front approaches the right surface with a decreasing velocity, and the phase-change process is then completed. The heat transfer mechanism reverts into steady-state process at this stage, and consequently, the heat flux on left side decreases to the value of the right side one. This situation explains

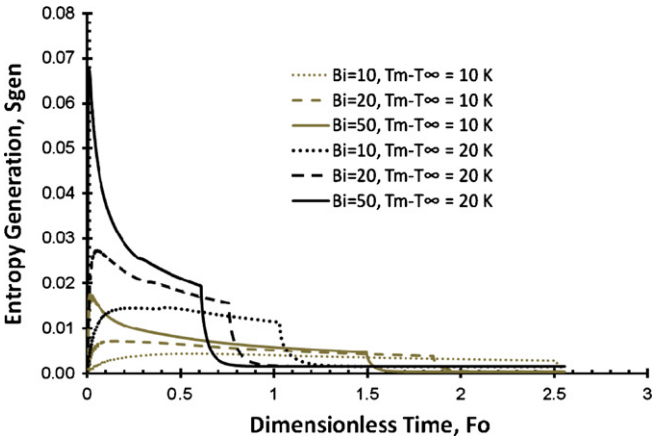

Fig. 7. The entropy generation with time for different Biot number (*Bi*) and temperature difference ($T_m - T_\infty$).

why the entropy generation suddenly decreases to its lowest value when the solidification process is almost completed. After that point, it starts decreasing slowly until the solidification process almost finishes completely and then it becomes zero suddenly. Entropy generation rises with increasing heat flux on the right side of channel and it is not reaching to zero at the right side of channel in the case of applying a non-zero heat flux.

Entropy generation curves with respect to dimensionless time, based on different Biot number and temperature difference, are illustrated in Fig. 7. At constant temperature difference of $\Delta T = 10$ or 20 K, entropy generation rises when Biot number is increased. And similarly, at constant Biot number, entropy generation is directly proportional to temperature difference.

5. Conclusions

A comprehensive thermodynamic analysis, incorporating the entropy generation in heat conduction, of a parallel plate channel phase-change flow accompanied by melting/solidification has been performed. The energy and entropy equations for one-dimensional transient thermal analysis with associated boundary and initial conditions have been solved numerically using a fixed grid numerical model with the finite control volume approach following the Thomas algorithm. This thermodynamic analysis of one dimensional flow allows several conclusions to be drawn. This information should assist efforts to understand the thermodynamic losses of one dimensional parallel plate channel phase-change flow and consequently to improve it.

The solidification fronts increase with time until it reaches 1, as it is a dimensionless parameter. Also the duration of complete solidification of channel increases while the heat flux on the hot site of the channel is increased.

The solidification takes place faster when environment temperature T_∞ at cold side of channel decreased, and the same effect is apparent when convection heat transfer coefficient h is increased and/or thermal conductivity k is decreased.

Entropy generation increases rapidly at the beginning and makes peak at inter-phase point. After that point, it is start decreasing slowly until the solidification process almost finishes completely and then it becomes zero suddenly. This is because entropy generation is higher in the solid part than the liquid part. Entropy generation rises with increasing heat flux on the right side of the channel and it is not reaching to zero on the right side of the channel in the case of applying a non-zero heat flux.

Acknowledgements

The authors acknowledge the support provided by their universities and the Natural Sciences and Engineering Research Council of Canada in Canada.

References

[1] H.S. Carslaw, J.C. Jaeger, Conduction of Heat in Solids, 2nd ed., Clearendon Press, London, 1959.
[2] A.Z. Sahin, I. Dincer, Int. J. Energy Res. 24 (2000) 1029–1039.
[3] M.N. Ozisik, Heat Conduction, John Wiley, 1980.
[4] S. Fukusako, N. Seki, Fundamental aspects of analytical and numerical methods on freezing and melting heat transfer problems, Annu. Rev. Numer. Fluid Mech. Heat Transfer 1 (1986), Ch 7.
[5] J. Crank, Free and Moving Boundary Problems, Clearendon Press, Oxford, 1984.
[6] Y. Cao, A. Faghri, W.S. Chang, Int. J. Heat Mass Transfer 32 (7) (1989) 1289–1298.
[7] J.S. Hsiao, B.T.F. Chung, ASME Paper No.84-Ht-2 (1984).
[8] Y. Cao, A. Faghri, J. Heat Transfer 112 (1990) 812–816.
[9] G.F. Naterer, Numer. Heat Transfer B 37 (2000) 393–414.
[10] P. Napson, Renew. Energy 30 (2005) 1345–1357.
[11] İ. Dağtekin, H.F. Öztop, A.Z. Şahin, Int. Heat Mass Transfer 48 (2005) 171–181.
[12] B.S. Yılbas, M. Pakdemirli, Heat Transfer Eng. 26 (10) (2005) 80–86.
[13] T. Kousksou, F. Strub, J.C. Lasvignottes, A. Jamil, J.P. Bedecarrats, Solar Energy Mater. Solar Cells 91 (2007) 1275–1281.
[14] S.V. Patankar, Numerical Heat Transfer and Fluid Flow, Hemisphere Publishers, 1980.